Am J Cancer Res 2023;13(8):3401-3416
www.ajcr.us /ISSN:2156-6976/ajcr0151580

Original Article

Yulangsan polysaccharide inhibits epithelial-mesenchymal transition and invasion in NSCLC by attenuating the TGF-β1/ERK signaling pathway

Feifeng Lan[1*], Menghua Chen[1*], Xiaowei Xie[1], Yanyan Mo[1], Fengti Chen[1], Renbin Huang[2], Wenqi Liu[1]

[1]*Department of Radiation Oncology, The Second Affiliated Hospital of Guangxi Medical University, Nanning 530007, Guangxi, China;* [2]*Pharmaceutical College, Guangxi Medical University, Nanning 530021, Guangxi, China.* [*]*Equal contributors.*

Received June 4, 2023; Accepted July 17, 2023; Epub August 15, 2023; Published August 30, 2023

Abstract: Active polysaccharides have unique advantages in inhibiting cancer cell proliferation, invasion and metastasis and inducing apoptosis. Yulangsan polysaccharide (YLSPS) is derived from the root of *Millettia pulchra* var. *laxior* (Dunn) Z. Wei. Previous studies revealed that YLSPS exhibits bioactivities such as antibacterial, antidepressive, antitumor, hepatoprotective and immunomodulating activities. However, the anticancer effects of YLSPS on lung cancer have not yet been studied, and its mechanism of action remains unclear. The present study investigated the anti-migration/invasion effects of YLSPS and possible mechanisms in lung cancer cells (A549 and Lewis) *in vitro* and *in vivo*. The data suggested that YLSPS reversed epithelial-mesenchymal transition (EMT) and inhibited the invasion and migration of lung cancer cells by inhibiting the TGF-β1-induced ERK signaling pathway. Furthermore, YLSPS reduced the levels of proteins associated with EMT, including vimentin, but increased those of E-cadherin, as determined by Western blotting. *In vivo*, YLSPS significantly inhibited the growth of xenograft tumors, and decreased the levels of TGF-β1 and protein markers associated with EMT. Importantly, YLSPS had fewer toxic side effects than cisplatin. Overall, YLSPS significantly delayed non-small cell lung cancer (NSCLC) progression by modulating EMT and TGF-β1/ERK signaling pathway. The present findings suggest that YLSPS may be a potential adjuvant therapy and drug for improving the tumor microenvironment of lung cancer.

Keywords: Yulangsan polysaccharide, NSCLC, epithelial-mesenchymal transition, migration, invasion, TGF-β1/ERK

Introduction

The majority of lung cancer cases are non-small cell lung cancer (NSCLC) and are diagnosed at an advanced stage. The 5-year survival rate for NSCLC is only 15% [1, 2]. Although immunological and targeted therapy of NSCLC has made great progress, problems of immune escape, radiotherapy resistance and targeted drug resistance lead to tumor metastasis and recurrence, which have become major problems in the treatment of NSCLC [3]. The increasing importance of epithelial-mesenchymal transition (EMT) in cancer progression and drug resistance in cancer cells requires its use as a starting point to identify targets for the EMT process and to develop therapeutic strategies for cancer invasion and metastasis. More importantly, there is also a need for further exploration of regulatory targets and mechanisms associated with NSCLC development.

There is evidence to suggest that the invasion and dissemination of cancerous cells occurs via EMT during metastasis [4-6]. EMT is characterized by a loss of the epithelial marker E-cadherin, an increase in mesenchymal markers (vimentin and N-cadherin), and an increase in migratory and invasive behavior [7]. TGF-β is a key cytokine in the tumor microenvironment that is influential in tumor progression. In addition to regulating the migration, proliferation and differentiation of cells, the TGF-β signaling pathway also regulates various other processes

[8], including induction of EMT, which is an important transdifferentiation process that allows epithelial cells to develop a mesenchymal phenotype, which then promotes tumor progression [9]. Numerous factors have led to the frequent failure of TGF-β pathway-related drugs, which prompted our group to investigate the mechanisms of TGF-β pathway-related drugs in greater depth; we also utilized tools such as bioinformatics and single-cell sequencing and information on targeted agents to identify candidate drugs.

Millettia pulchra var. *laxior* (Dunn) Z. Wei produces a highly effective extract called Yulangsan polysaccharide (YLSPS) [10]. As a well-known Zhuang medicine in Guangxi, YLSPS has various therapeutic properties, such as antifibrosis [11], antiinflammatory, liver protection [12-14], immunity enhancement [15, 16], nervous system protection [17, 18] and antitumor effects. Importantly, YLSPS has recently attracted considerable attention for its antitumor activity since its toxicity and safety profiles are better than those of chemotherapy agents [19]. YLSPS significantly inhibited proliferation and induced apoptosis in a human hepatoma carcinoma cell line in a dose-dependent manner, and the mechanism of action was associated with G_2/M cycle arrest [20]. It was found that the tumor suppression rates of the YLSPS low-, medium- and high-dose groups, which were also treated with cyclophosphamide (CTX), were 67.4, 76.1 and 74.8%, respectively, and YLSPS significantly increased the thymus and spleen indexes of mice with sarcoma, which led to significant potentiation and toxicity reduction effects in combination with CTX [21, 22]. In addition, it was previously found that serum containing YLSPS significantly inhibited the proliferation of breast cancer 4T1 cells and induced apoptosis, which was mainly associated with the inhibition of Bcl-2 and the promotion of Bax and caspase-3 protein expression. *In vivo* experiments revealed that the average tumor suppression rates for subcutaneously transplanted tumors in the YLSPS low-, medium- and high-dose groups were 18.41±0.86, 30.92±1.66, and 38.84±1.04%, respectively, indicating that the compound could enhance the regulatory effect of immune cells and stimulate antiangiogenesis [23]. However, there are currently no reports illustrating its anti-migratory/invasive properties in NSCLC.

YLSPS has been reported to have antitumor effects. However, the currently available information is not sufficient to justify the use of YLSPS in the clinical treatment of cancer. Its mechanism and effect in NSCLC have yet to be determined. The study used YLSPS-containing serum for *in vitro* experiments and established a mouse Lewis cell-loaded tumor model for *in vivo* experiments to evaluate the reversal effect of YLSPS on EMT in NSCLC, with the aim of providing data for the development of natural drugs against lung cancer and a scientific basis for guiding clinical treatment.

Materials and methods

YLSPS-containing serum preparation

YLSPS was acquired by Professor Renbin Huang and was prepared by a method described previously [10]. A total of 50 SD rats weighing 180-220 g were provided by the Experimental Animal Center of Guangxi Medical University (SYXK2020-0004). Experimental rats were randomly divided into five groups: control group; positive control (CDDP) group; low-dose YLSPS group (750 mg/kg/day); medium-dose YLSPS group (1,500 mg/kg/day); and high-dose YLSPS group (3,000 mg/kg/day). YLSPS was administered orally twice daily. For the negative control, the animals were treated with distilled water via gavage; for the positive control, CDDP was injected intraperitoneally at 8 mg/kg every 2 days. A blood sample was obtained from the abdominal aorta of rats 1 h after the last injection following 7 days of treatment (under anesthesia with 2% pentobarbital sodium intraperitoneally at 40-50 mg/kg). Upon centrifuging the whole blood for serum isolation, the sample was filtered through a cellulose acetate membrane of 0.22 μm. The serum was then inactivated at 56°C for 30 min and stored at -20°C [23].

Reagents

FBS was purchased from Shanghai Shuangru Biotechnology. High-glucose DMEM was provided by Gibco, while a penicillin-streptomycin mixture and 0.25% trypsin-EDTA digestion solution were purchased from Beijing Solarbio Science & Technology. Cell Counting Kit-8 (CCK-8) was obtained from Biosharp Life Sciences. Recombinant human TGF-β1 powder

(PeproTech) was dissolved in 4 mM HCl containing 1 mg/ml (stock, 10 μg/ml). The ERK inhibitor U0126 and agonist TBHQ were purchased from MCE. Matrigel basement membrane matrix was acquired from BD Biosciences, while Transwell plates were acquired from Corning. Universal tissue fixative was purchased from Biosharp Life Sciences. Anti-ERK, anti-Snail and anti-E-cadherin antibodies were purchased from CST, while anti-vimentin and phosphorylated (p)-ERK antibodies were purchased from Santa Cruz Biotechnology.

Cell viability assay

The human NSCLC A549 cell line and the mouse lung cancer cell line Lewis were provided by Procell Life Science & Technology. A549 and Lewis cells in logarithmic growth phase were seeded at a density of 3×10^4/ml in 96-well plates with 100 μl culture medium per well and three replicate wells per set. After cell attachment, the cells were treated with medium containing different concentrations of YLSPS for 24, 48 and 72 h. Next, 10 μl CCK-8 and 90 μl DMEM were added to each well. After incubation at 37°C in the dark for 2 h, the absorbance was measured at 450 nm using a microplate reader (Thermo Fisher Scientific).

Analysis of EMT alterations in TGF-β1-stimulated cells

We treated A549 and Lewis cells with 10 ng/ml TGF-β1 for 48 h to observe the changes in cell morphology [24-26]. Western blotting was also applied to detect alterations in EMT-related proteins. According to the CCK-8 experimental results, the most appropriate dose of drug-containing serum was selected for subsequent experiments.

Wound healing assay

The cells were subjected to the following three treatments: i) Blank serum control group; ii) TGF-β1 group (with blank serum and 10 ng/ml TGF-β1); and iii) TGF-β1 + YLSPS-containing serum group. A549 and Lewis cells in logarithmic growth phase were separately resuspended and inoculated into 6-well plates per well (5×10^5 cells). TGF-β1 was also added and incubated for 48 h. When cells adhered to the wall, a scratch was created with a 200-μl pipette tip, followed by three washes with PBS. After 24/48 h of treatment with YLSPS-containing serum, the width of the scratch was observed and photographed [27].

Transwell-migration/invasion assay

The vertical migration and invasion of lung cancer cells were evaluated by Transwell assays using 24-well plates (0.8-μm pore size). Cells were pretreated with blank serum and YLSPS-containing serum for 48 h, and then a total of 1×10^4 cells were seeded into the upper chamber in serum-free DMEM. The lower chamber was filled with 600 μl DMEM containing 10% FBS as a chemoattractant. After culturing for 24 h, the non-invading cells were removed from the upper surface of the membrane. The migrated cells on the lower surface were fixed with 4% formaldehyde for 30 min and stained with crystal violet for 5 min. The number of cells in 6 fields of each triplicate filter was counted. Cell invasion assays were performed in a similar manner, with the following exception 5×10^4 cells with Matrigel diluted in serum-free DMEM (1:8) were seeded into the upper inserts.

Western blotting

A549 and Lewis cells were induced with TGF-β1 to undergo EMT according to the aforementioned method and grouping, and then the cells were treated with drug-containing or drug-free serum-containing medium for 48 h. Prior to the experiment, it was hypothesized that YLSPS regulates the invasion and migration of NSCLC through the TGF-β1/ERK signaling pathway. Next, the cells were washed with cold PBS and lysed with RIPA buffer and PMSF according to the manufacturer's protocol. The cells were then centrifuged at 13,000 rpm for 15 min at 4°C. Next, protein concentrations were determined by BCA assay. Samples (20-30 μg/lane) were then subjected to 8-16% SDS-PAGE and transferred onto PVDF membranes. After blocking with 5% nonfat dry milk in TBS containing 0.1% Tween-20 (TBST) buffer for 2 h at room temperature, the membranes were incubated overnight at 4°C with the corresponding diluted primary antibodies: anti-E-cadherin (1:1000), anti-vimentin (1:1000), anti-snail (1:1000), anti-ERK (1:1000), and anti-p-ERK (1:500). The β-actin signals were used to normalize the band signals (1:1000). After three washes with 1× TBST buffer, the membranes were incubat-

ed with HRP-conjugated secondary antibody (1:5000) at room temperature for 2 h. Upon washing three times with 1× TBST buffer, the protein bands were detected via enhanced chemiluminescence.

Immunofluorescence staining

A549 and Lewis cells were treated with the ERK activator TBHQ (10 μM) alone or in combination with YLSPS-containing serum. Cells were fixed with 4% paraformaldehyde for 30 min and permeabilized with 0.3% Triton X-100 for 20 min at room temperature, followed by three washes with PBS. Next, the samples were blocked with 5% goat serum for 2 h, and incubated with anti-ERK (1:800) and anti-p-ERK (1:100) antibodies overnight. Antibodies were washed off with PBS, and the samples were then incubated with goat anti-rabbit IgG (H+L) (1:100) for 2 h. PBS was used for washing three times, and the slides were then sealed with anti-fluorescence quencher containing DAPI. Finally, the cells were observed under a fluorescence microscope and photographed. The fluorescence intensity of the stained cells was calculated by ImageJ software.

Tumor xenograft model and in vivo YLSPS treatment

The experiment was conducted at the Animal Research Facility of Guangxi Medical University. Consent for all operations was obtained from the Ethics Committee. Female C57BL/6J mice (18-20 g) were adaptively fed for 1 week in a relatively pathogen-free environment. Tumor-bearing mice were generated by injecting 0.1 ml 2 × 10^6/ml Lewis cells into the right axilla of C57BL/6J mice. When the tumors became visible, the animals were divided into four groups for the following treatments: control group: administered distilled water; CDDP group: intraperitoneal injection of 2 mg/kg CDDP every 2 days as a positive control; YLSPS high group: injection of 1,200 mg/kg YLSPS once per day; YLSPS low group: injection of 600 mg/kg YLSPS once per day. The tumor volume was measured by Vernier calipers every 2 days and calculated with the formula length × width^2 × 0.5. After 14 days of rearing, the tumors were excised, photographed and weighed. Tumor samples were fresh-frozen and stored at -80°C, and at the same time, a part of the tissue was fixed in paraformaldehyde fixation solution for subsequent analysis.

Hematoxylin and eosin (H&E) staining

Tumor tissue was fixed in 4% paraformaldehyde and paraffin embedded, and the wax blocks were cut into 5 μm-thick sections, dewaxed, hydrated, and stained with hematoxylin. Multiple steps including washing, eosin solution, dehydration, transparency and sealing, were performed to prepare the sections. Next, pathological changes were observed by light microscopy, photographed at ×400 magnification, and scored based on the degree of necrosis.

Immunohistochemistry (IHC)

Paraffin-embedded tissues were sectioned, dewaxed and subjected to antigen retrieval by boiling in a pH 6.0 citrate buffer containing 10 mM citrate and then deparaffinized again. The next steps were performed overnight at 4°C: 3% H_2O_2 was used to block endogenous peroxidase, and then the sections were blocked with nonimmune serum and incubated with antibodies against E-cadherin (1:400), vimentin (1:500), TGF-β1 (1:200), Ki67 (1:200), Snail (1:400), ERK (1:100) and p-ERK (1:50). After incubation with goat anti-rabbit (1:200), staining with DAB chromogen and counterstaining with hematoxylin, the slides were analyzed under a light microscope.

Reverse transcription-quantitative PCR (RT-qPCR) analysis

Total RNA was extracted with TRIzol® reagent following the manufacturer's instructions. RNA was reverse transcribed into cDNA using HiScript IIIRT SuperMix for qPCR (+gDNA eraser) (Vazyme Biotech) using ChamQ Universal SYBR qPCR Master Mix according to the manufacturer's instructions on a 7,500 system (Thermo Fisher Scientific). The relative fold changes in mRNA were determined by using the $2^{-\Delta\Delta Ct}$ method, using GAPDH as the endogenous control. The primers for PCR were as follows: E-cadherin forward 5'-ACTTTGGTGTGGGTCAGGAA-3' and reverse 5'-CACATGCTCAGCGTCTTCTC-3'; vimentin forward 5'-CGCTTTGCCAACTACATCGA-3' and reverse 5'-CCTCCTGCAATTTCTCTCGC-3'; and GAPDH forward 5'-ATGGTGAAGGTCGGTGTGAA-3' and reverse 5'-TGGAAGATGGTGATGGGCTT-3'.

Statistical analysis

GraphPad Prism 9 and SPSS 26 software were used for statistical analyses. Differences between different treatment groups were analyzed by one-way ANOVA. $P<0.05$ was considered to indicate a statistically significant difference.

Results

YLSPS inhibits the proliferation of A549 and Lewis cells

The viability of A549 and Lewis cells decreased with increasing YLSPS serum concentrations, with a more pronounced inhibitory effect in the YLSPS high-dose group (**Figure 1A**). However, the YLSPS-containing serum did not significantly inhibit cell viability with increasing times, and the effect was particularly weak at 72 h (**Figure 1B**). Based on the results of the CCK-8 experiment, serum from the YLSPS high-dose group was used for the follow-up experiment, and the intervention time was 48 h. The results suggested that YLSPS-containing serum could effectively inhibit the proliferation of A549 and Lewis cells.

TGF-β1 induces EMT in cells

A549 and Lewis cells were treated with TGF-β1 for 48 h to observe changes in cell morphology, and it was found that TGF-β1 induced changes in cell morphology from polygonal to fibroblast-like and spindle-like mesenchymal morphology compared with control group cells (**Figure 1C**). In both types of cells treated for 48 h, TGF-β1 decreased E-cadherin protein levels and increased vimentin protein levels, as determined by Western blotting (**Figure 1D**). These data suggest that TGF-β1 induced EMT changes in lung cancer cells, indicating that our model was successfully established.

The migration and invasion of NSCLC cells can be inhibited by serum containing YLSPS

EMT changes in the cells were first induced with TGF-β1, followed by treatment with blank or YLSPS-containing serum to evaluate the effect of YLSPS on the migration of cells by wound healing assay (**Figure 2A**). The data showed that the lateral migration ability of cells in the TGF-β1 group was significantly enhanced and the cell migration rate was significantly increased compared with that in the control group, while treatment with YLSPS-containing serum inhibited the migration of lung cancer cells (**Figure 2B**). Prior to Transwell migration and invasion assays, cells were treated with blank and YLSPS-containing serum, and then induced with TGF-β1. The longitudinal migration and invasion of A549 and Lewis cells were significantly enhanced by TGF-β1. Importantly, this enhancement was attenuated by serum-containing YLSPS (**Figure 3**).

YLSPS affects the expression of EMT-related markers in NSCLC cells induced by TGF-β1 by blocking the TGF-β1/ERK signaling pathway

YLSPS-containing serum inhibited the invasion and migration of lung cancer cells. Western blotting assays were employed to further investigate the mechanism by which YLSPS affects NSCLC cells. The results showed that the YLSPS-containing serum and ERK inhibitor group exhibited increased expression of E-cadherin, indicating that this treatment attenuated the effects of TGF-β1 induction. However, YLSPS-containing serum and inhibitor U0126 inhibited the induction of vimentin and Snail expression by TGF-β1 in NSCLC cells (**Figure 4A**). Assays for TGF-β1/ERK pathway-related factors revealed that YLSPS-containing serum had no significant effect on the protein expression of total ERK, while p-ERK protein levels were significantly decreased, acting in the same way as the pathway inhibitor, suggesting that YLSPS may inhibit the EMT process in lung cancer by blocking the TGF-β1/ERK signaling pathway (**Figure 4B**). Immunofluorescence analysis showed that the ERK activator TBHQ increased the expression of p-ERK, while treatment with YLSPS-containing serum partially reversed ERK phosphorylation and thus decreased p-ERK expression, but had no significant effect on total ERK protein. These results suggested that YLSPS effectively inhibited ERK phosphorylation in lung cancer cells (**Figure 5**).

Analysis of C57BL/6J mice bearing lung cancer showed that YLSPS inhibited tumor growth and increased histopathological damage

C57BL/6J mice were subcutaneously injected with Lewis cells to verify the accuracy of the *in vitro* experiments. The results showed that the

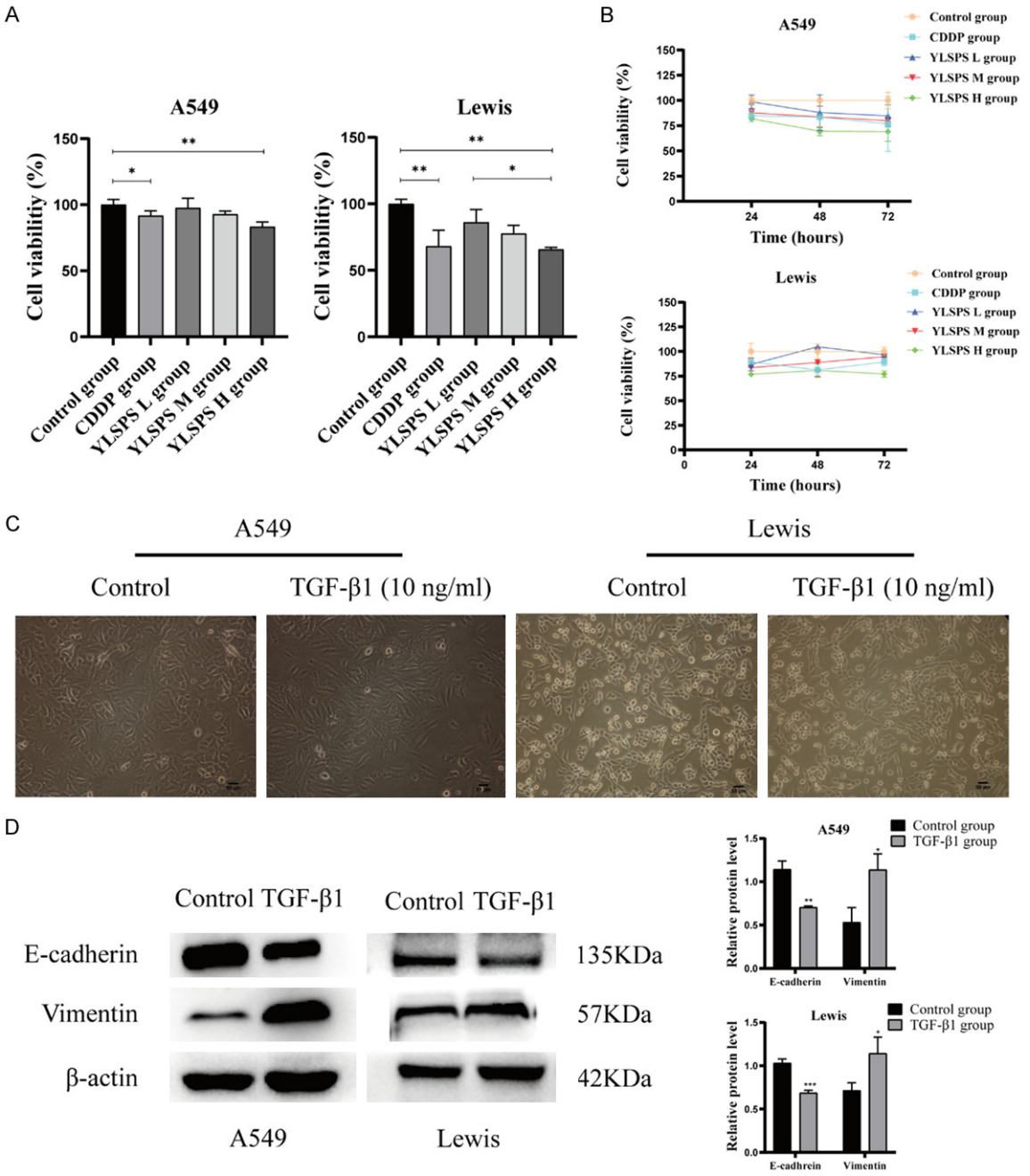

Figure 1. TGF-β1 influences epithelial-mesenchymal transition in A549 and Lewis cells. A. Cell viability of A549 and Lewis cells. B. Cell viability at different time points. C. A549 and Lewis cells were treated with TGF-β1 at a concentration of 10 ng/ml (Scale bar =50 μm). D. Western blot analysis of E-cadherin and vimentin levels in A549 and Lewis cells treated with TGF-β1 (10 ng/ml) for 48 h compared with the control group. Data are presented as the mean ± SD (n=3), *, $P<0.05$, **, $P<0.01$.

tumor growth rate increased from the seventh day of intervention, while cisplatin and high-dose YLSPS significantly inhibited tumor growth (**Figure 6A**, **6B**). From the seventh day, the mice in the cisplatin group gradually lost body weight, and the difference in body weight between this group and the control group was significant, while the mice in the YLSPS low- and high-dose groups did not show significant changes in body weight. This indicates that YLSPS is safe and effective in tumor treatment (**Figure 6C**, **6D**).

Based on the H&E staining results, the control group's tumor tissues were structurally and

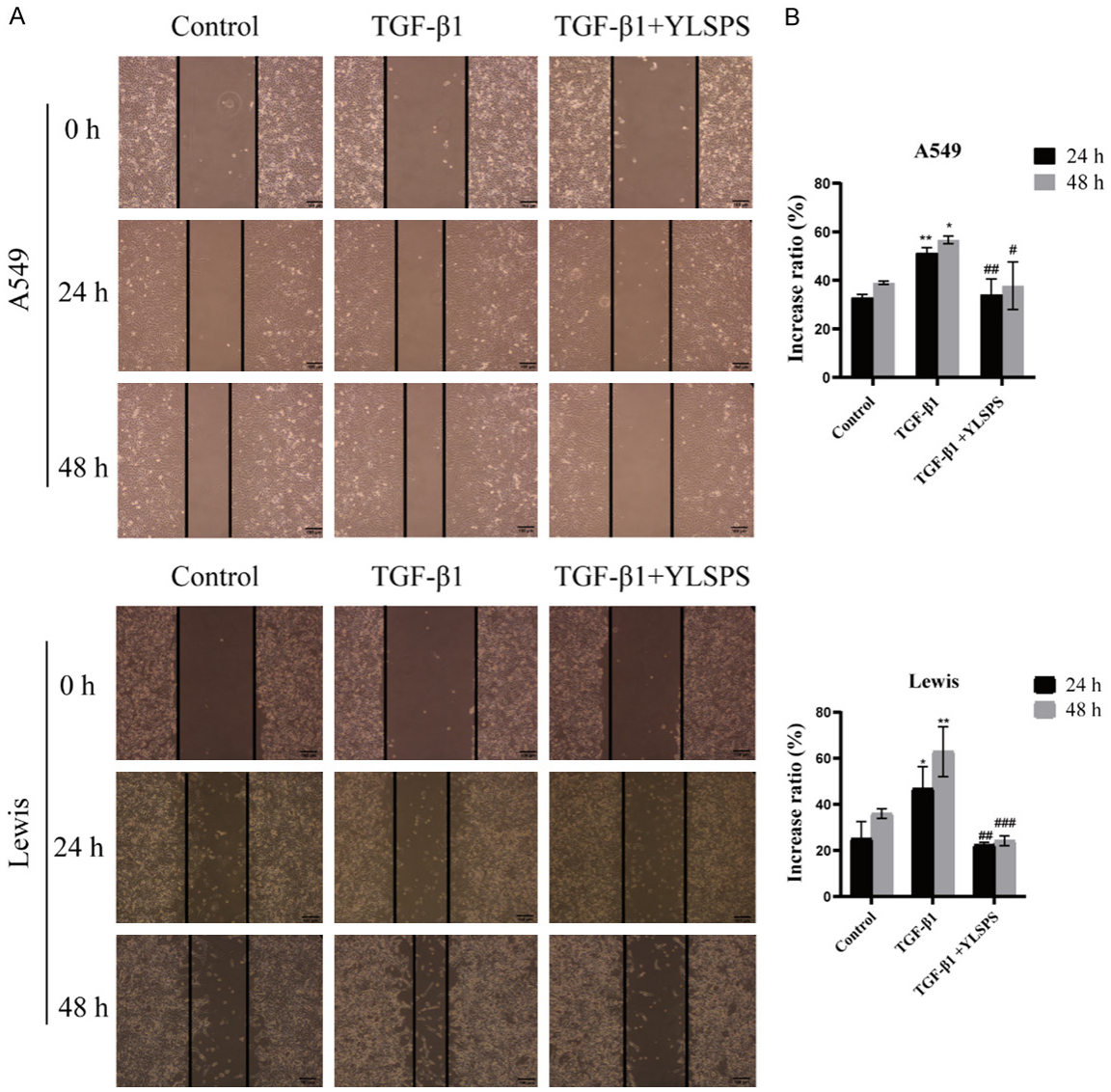

Figure 2. *In vitro* migration of A549 and Lewis cells with serum-containing YLSPS was evaluated by (A) wound healing and (B) quantitative assays. All values are presented as the mean ± SD (n=3) (Scale bar =100 μm). *, $P<0.05$ vs. the control group, #, $P<0.05$ vs. the TGF-β1 group.

morphologically intact, while the tumor tissues in the other treatment groups presented varying degrees of necrosis. The tumor volume was smaller and the area of necrosis was the largest in the cisplatin group, followed by the YLSPS high-dose group, suggesting that the cisplatin group had the best inhibitory effect on tumor growth (**Figure 6E**). Tissues from each group were compared according to the tumor tissue damage scoring criteria, and the tumor tissue damage scores were significantly higher in the cisplatin and YLSPS groups than in the control group (**Table 1**).

YLSPS restrains the expression of TGF-β1 and EMT-related markers in Lewis tumor-bearing mice

To verify the expression of EMT-related proteins such as E-cadherin, vimentin, TGF-β1 and Ki67 *in vivo*, IHC and RT-qPCR were performed in tumor tissues of mice. IHC showed that the positive expression rate of E-cadherin protein was increased in the YLSPS and CDDP groups, while treatment with YLSPS and cisplatin attenuated the positive expression of vimentin, Ki67 and TGF-β1 protein (**Figure 7A**). The effect of YLSPS

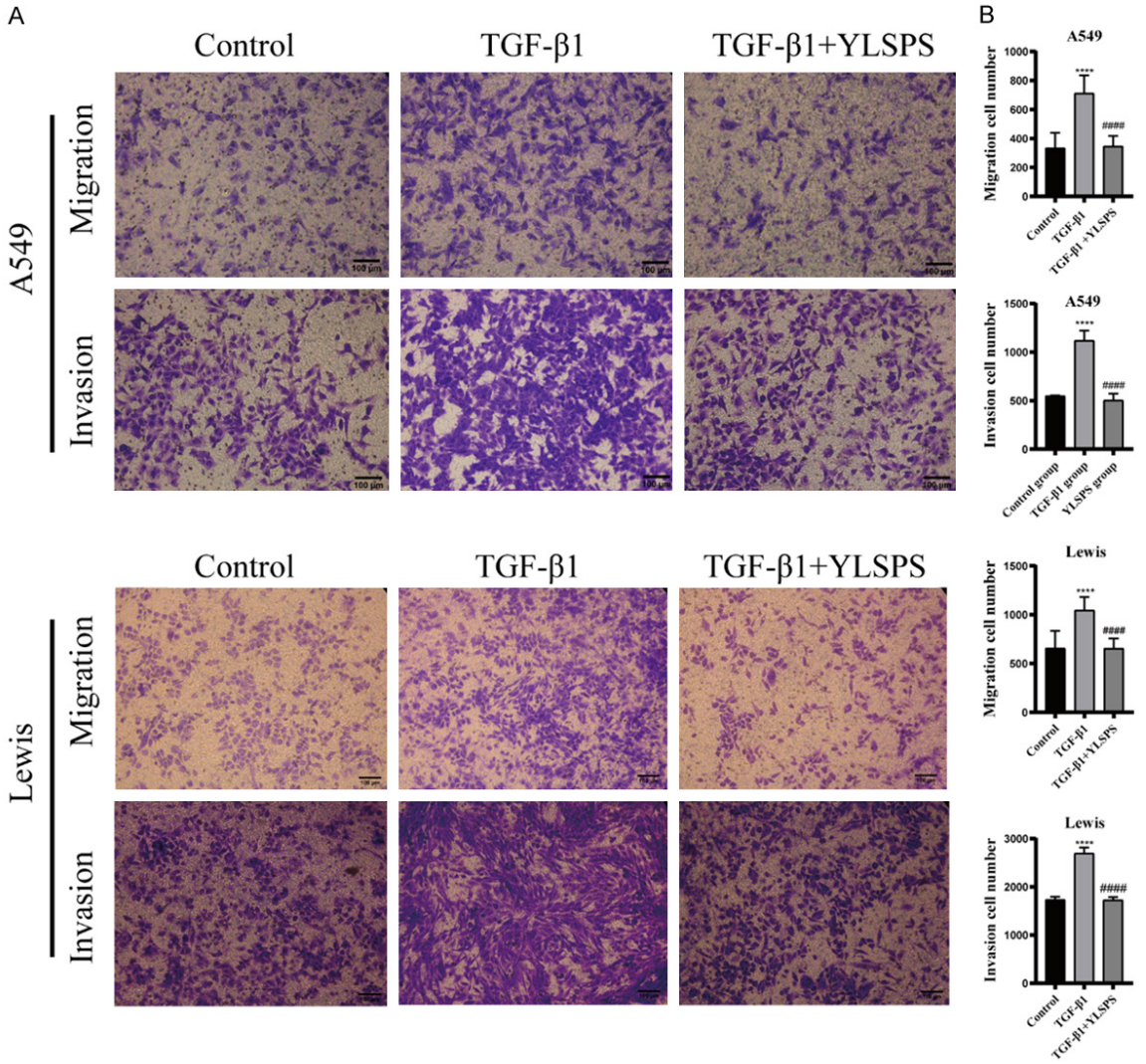

Figure 3. YLSPS in serum attenuates the enhancement of tumor cell migration and invasion induced by TGF-β1. A. The effects of serum containing YLSPS on the migration and invasion of A549 and Lewis cells were examined by Transwell assays. B. Statistical analysis of the migrated and invaded cell numbers in A549 and Lewis cells. Data are presented as the mean ± SD (n=3) (Scale bar =100 μm). *, $P<0.05$ vs. the control group, #, $P<0.05$ vs. the TGF-β1 group.

on the ERK signaling pathway *in vivo* was detected by IHC, and the results showed that the expression of p-ERK and Snail in tumor tissues was attenuated after treatment with YLSPS and cisplatin, but the expression of ERK was not significantly changed, which was consistent with the results of the *in vitro* experiments (**Figure 8A**).

RT-qPCR was used to determine the transcription levels of EMT-related factors. The results showed that YLSPS increased the mRNA level of E-cadherin and downregulated the mRNA level of vimentin compared with the control group (**Figure 7B**). In addition, the effect of YLSPS on tumor invasiveness was also investigated, and lungs from tumor-bearing mice were harvested to observe lung metastases after YLSPS and cisplatin treatment. According to the pathological results of lung tissues, metastasis of cancer cells was found in the lung tissues of the control group, while no cancer cells were found in the YLSPS or cisplatin groups (**Figure 8B**).

Discussion

Natural products have long been a part of traditional Chinese medicine (TCM) and have played an instrumental role in the development of anti-

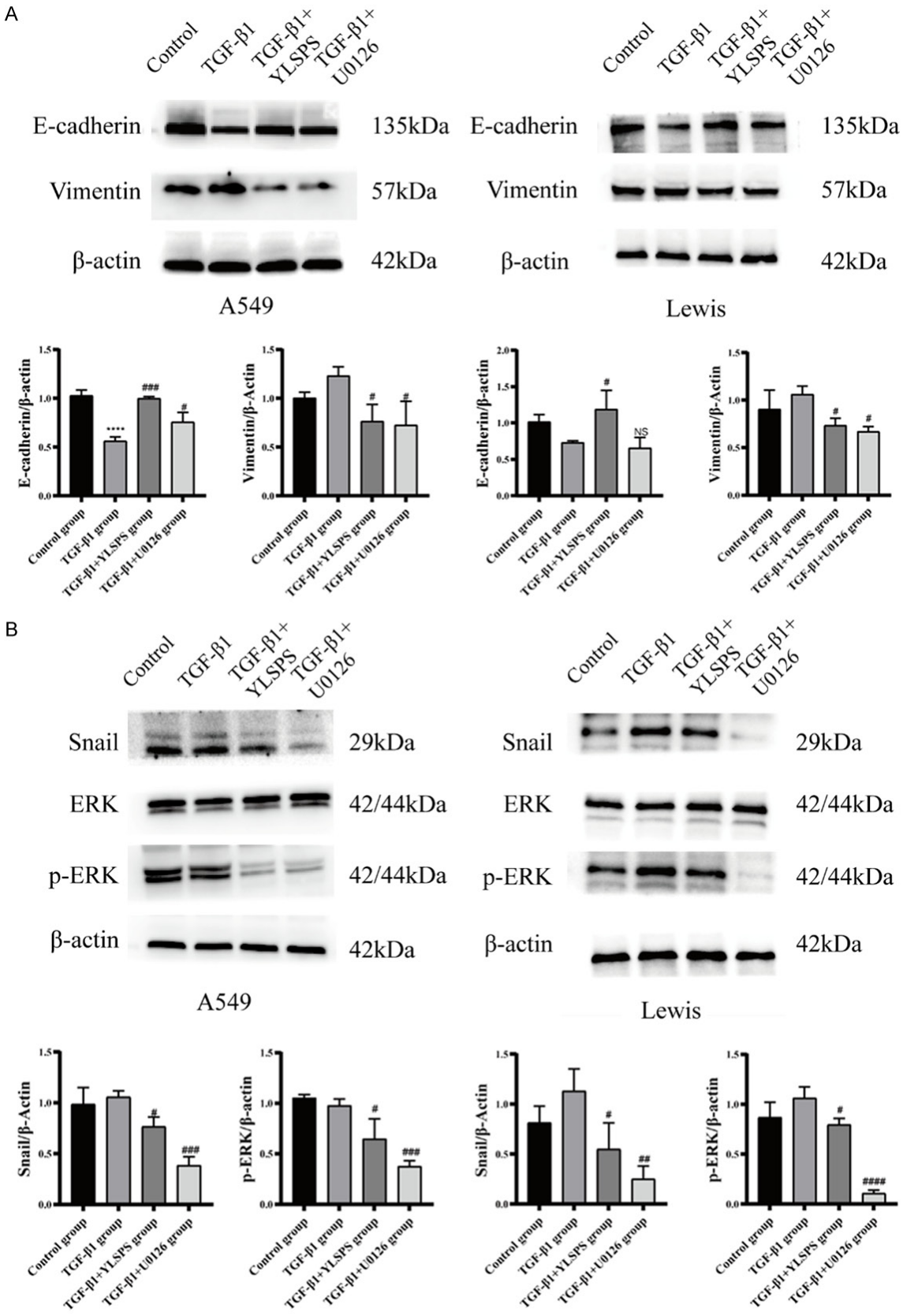

Figure 4. EMT-related markers and the TGF-β1/ERK signaling pathway were suppressed in A549 and Lewis cells stimulated with TGF-β1 and treated with serum containing YLSPS. A. Western blotting detected the EMT-related pro-

tein levels of cells. B. The expression of ERK, phosphorylated ERK and Snail was detected after cell treatment with serum-containing YLSPS. Data represent the mean ± SD (n=3), #, *P*<0.05 vs. the TGF-β1 group.

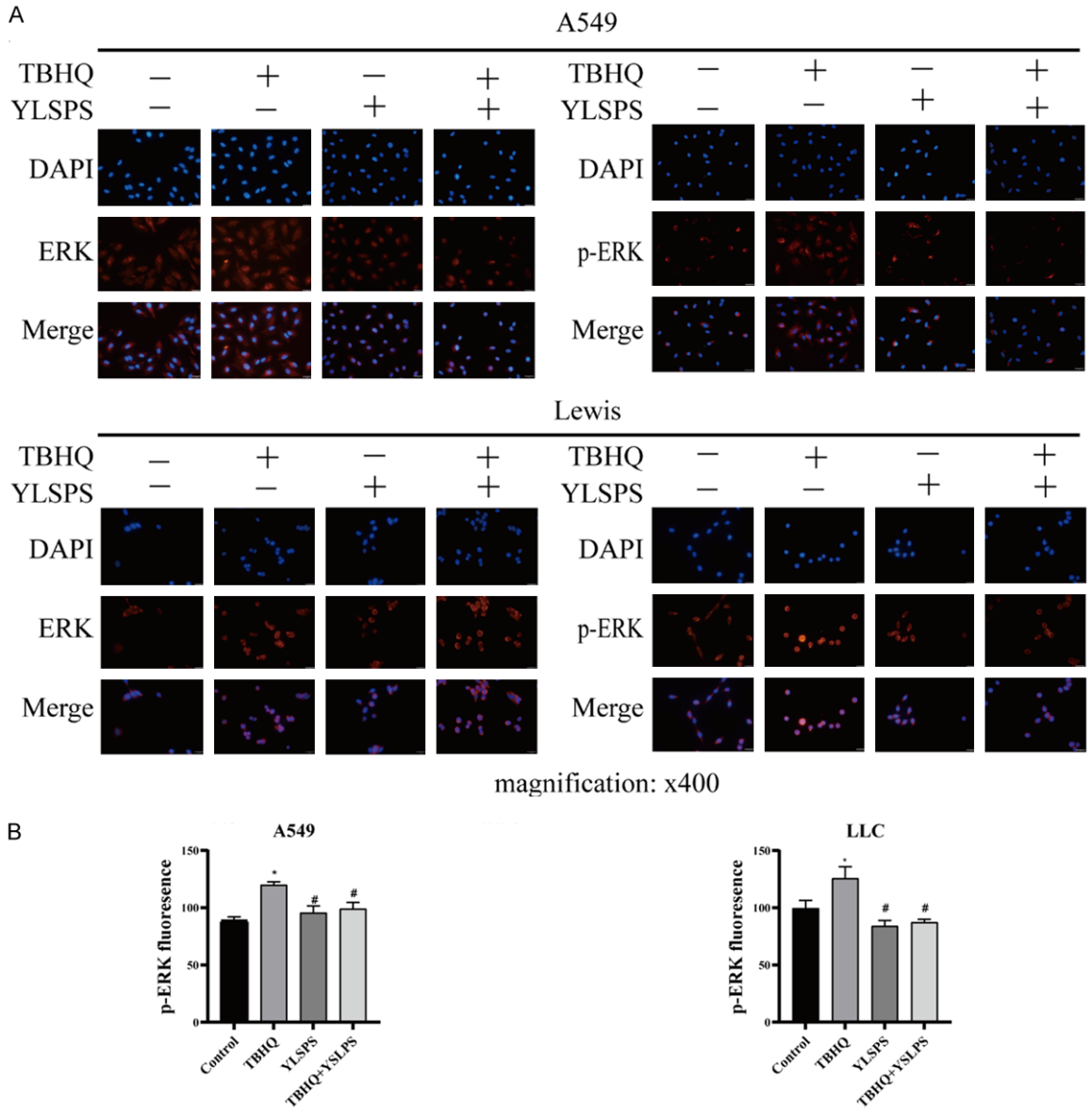

Figure 5. A. Immunofluorescence staining was performed to detect ERK and phosphorylated ERK expression, which is shown in red, while the nuclei appear in blue (magnification: ×400). B. The fluorescence intensity of each group was calculated by ImageJ. Data represent the mean ± SD (n=6). *, *P*<0.05 vs. the control group, #, *P*<0.05 vs. the TBHQ group.

cancer drugs. Since TCM compounds generally have lower toxicity and incidence of side effects than chemotherapeutic drugs, the antitumor effect of TCM compounds and their ability to regulate the tumor microenvironment have attracted increased attention; thus, herbal medicines are important resources for developing new drugs [28]. The development of natural nontoxic macromolecules can be used as a new strategy for cancer treatment as well as an adjuvant treatment to regulate the internal environment of the human body [29, 30]. At present, the specific mechanisms of action of many TCM compounds remain poorly understood. In addition, the effects of TCM compounds are multitarget and complex. To date,

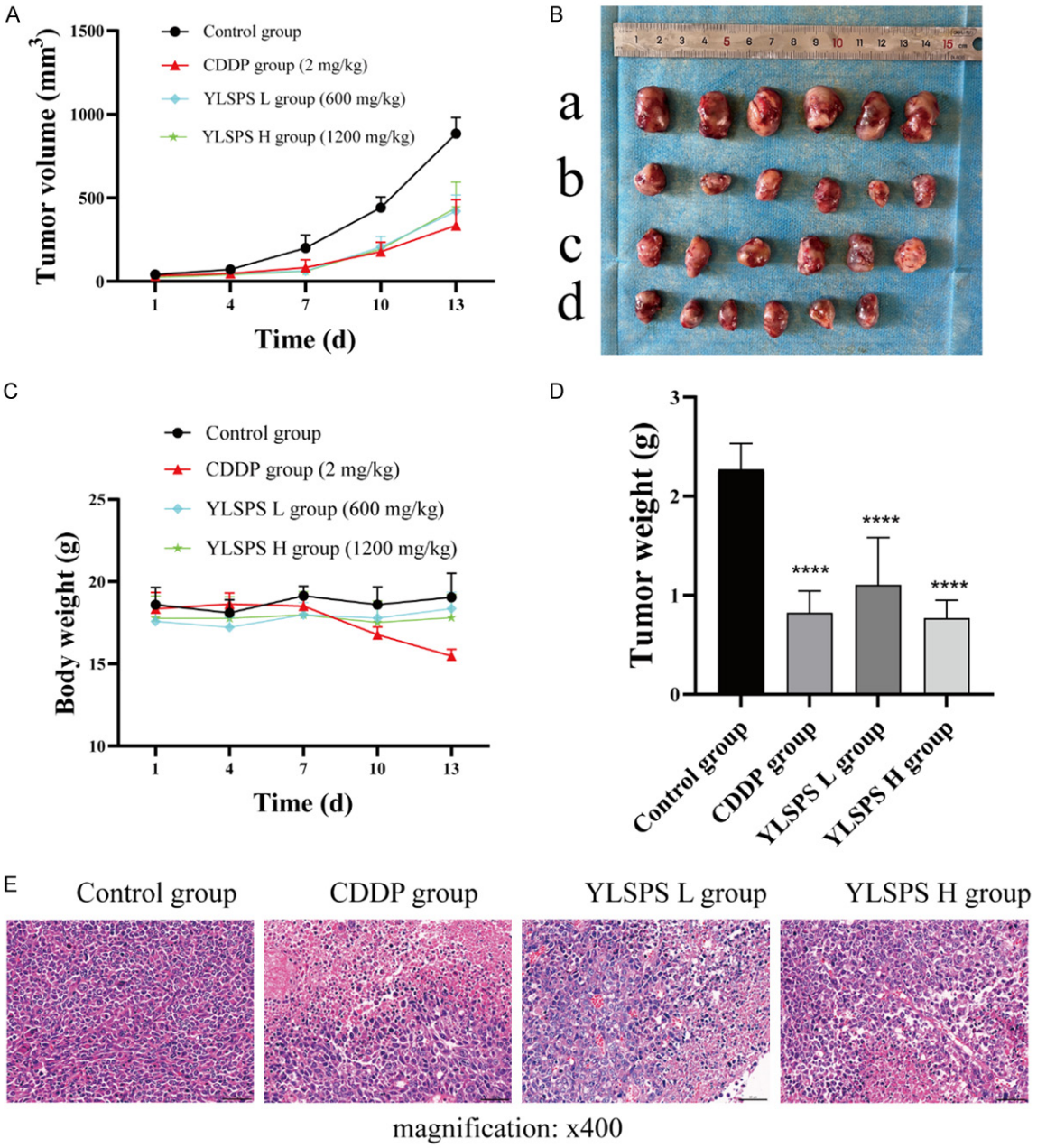

Figure 6. YLSPS attenuates tumor growth and promotes histopathological damage in tumor-bearing mice. A. Growth curve of tumor volume after initiation of intervention. B. Photograph of subcutaneous xenografts in C57BL/6J mice after 14 days of treatment with CDDP and YLSPS: (a) Control group; (b) CDDP (2 mg/kg); (c) YLSPS low-dose group (600 mg/kg); and (d) YLSPS high-dose group (1,200 mg/kg). C. Weight of mice in each group. D. Weight of xenografts in each group. All values are presented as the mean ± SD (n=6). *, $P<0.05$ vs. the control group. E. Hematoxylin and eosin staining was used to evaluate micrographs of xenografts (magnification: ×400).

the antitumor effect of YLSPS has been studied in several tumors, but it has not been reported whether YLSPS affects the migration or invasion of lung cancer cells. Thus, the present study investigated the effect of YLSPS on EMT in lung cancer for the first time.

Previous studies have shown that EMT confers a phenotype and cellular plasticity to tumor cells, resulting in a loss of epithelial-like cell polarity, reduced intercellular adhesion, and increased metastatic and invasive capacity, as evidenced by changes in the expression of cal-

Table 1. Tumor tissue damage score results and statistic ($\bar{x}$ ± SD)

Group	Number	$\bar{x}$ ± SD
Control group	6	0.00±0.00
CDDP group	6	2.67±0.52*
YLSPS Low group	6	2.00±0.89*
YLSPS High group	6	1.67±0.52**

Note: Groups CDDP, YLSPS L and H are compared with the control group, *, $P<0.05$, **, $P<0.01$.

reticulin (E-cadherin) and vimentin [31, 32]. The signaling pathways involved in EMT include Wnt/β-catenin, TGF-β and Notch, among others [33, 34]. TGF-β is an important factor in the immune microenvironment of tumors and has been intensively studied in recent years [35]. It is also an effective EMT inducer and can regulate the migration and invasion process of tumors through the classical TGF-β/Smad signaling pathway and nonclassical pathways such as the TGF-β/ERK signaling pathway [36, 37]. Since TGF-β1-induced EMT in tumor cells is a classic pathological model for the study of cancer cell metastasis and invasion, it was used as an inducer for the establishment of the lung cancer EMT model in this study. Consequently, reversing EMT may be an effective strategy for inhibiting cancer metastasis.

As an effective immunosuppressive factor, the immunosuppressive effect of TGF-β helps tumors evade the immunosurveillance function of normal organisms. Moreover, TGF-β can inhibit the proliferation and differentiation of a variety of immune cells in tumor tissues, as illustrated by its roles in inducing tumor-associated macrophage (TAM) and tumor-associated neutrophile (TAN) polarization, blocking dendritic cell maturation, promoting regulatory T-cell production, inhibiting T-cell proliferation and activation, recruiting Myeloid-derived suppressor cells (MDSCs) and enhancing the procancer effects of TGF-β signaling in the tumor microenvironment [38]. TGF-β plays an important role in tumor immune evasion; however, slow progress has been made in developing therapies that inhibit its signaling [39]. To elucidate the mechanism by which YLSPS inhibits lung cancer cell invasion and migration through downregulation of TGF-β1, the current study investigated signaling pathways frequently involved in tumorigenesis in human cancer. Multiple stimulus signals such as changes in protein concentration, internal metabolic stress, DNA damage pathways, cell-matrix interactions, external growth factors and signals from other cells, are often received by the MAPK/ERK signaling pathway, which is a convergent signaling node [40, 41]. Therefore, we showed that the TGF-β/ERK pathway was involved in the inhibitory effect of YLSPS on lung cancer cell migration and invasion by adding an ERK inhibitor (U0126) to serve as a control. *In vitro* results showed that TGF-β1 activated the ERK signaling pathway and that YLSPS reversed EMT in lung cancer cells by inhibiting ERK phosphorylation. The antimigration and invasive effects of YLSPS were further illustrated by the addition of an ERK activator (TBHQ) through the inhibition of ERK phosphorylation.

The results of *in vitro* experiments showed that the cells underwent significant morphological changes upon TGF-β1 stimulation; they changed from a polygonal to spindle shape and lost intercellular adhesion. The expression of E-cadherin, a marker protein of the epithelium, was also downregulated, while the expression of vimentin, a marker protein of the mesenchyme, was increased, indicating that both cell lines underwent the EMT process induced by TGF-β1. The current study examined for the first time the effect of YLSPS-containing serum on the development of migration and invasion of A549 and Lewis cells after TGF-β1 induction. The results of the cell functional assay showed that YLSPS-containing serum inhibited the migration and invasion abilities of TGF-β1-induced NSCLC cells, indicating that YLSPS had certain anti-lung cancer effects.

In vitro drug screens and *in vivo* subcutaneous xenograft models are conventional preclinical models used in cancer drug discovery [42]. It was shown that the MTD of YLSPS was 25,000 mg/kg and had no significant toxic effect [43]. C57BL/6J mice were implanted with subcutaneous tumors, and after 14 days of administration, the tumor volume in the YLSPS-treated group was lower than that in the control group, where the tumor suppression effect of the YLSPS high-dose group was the same as that of the CDDP group. More importantly, it had fewer toxic side effects and better safety than

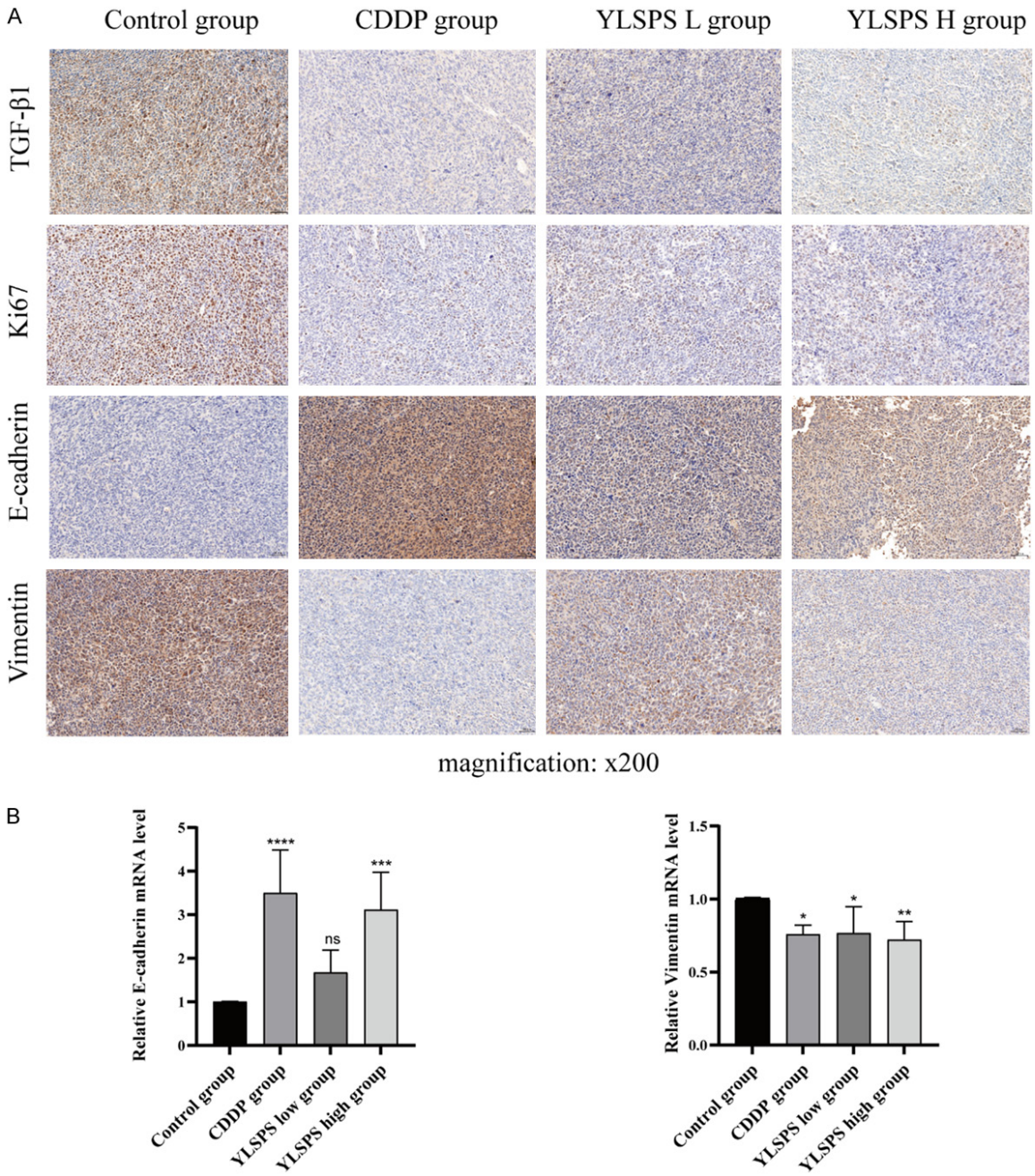

Figure 7. IHC and RT-qPCR of xenograft tumors. A. The expression of the EMT-related markers, TGF-β1 and Ki67 in Lewis tumor-bearing mice in each group (magnification: ×200). B. The vimentin and E-cadherin mRNA levels. Data represent the mean ± SD (n=6). *, *P*<0.05 vs. the control group.

CDDP, and the whole intervention process did not significantly affect the body weight of mice, while the body weight of mice in the cisplatin group decreased significantly, which is consistent with the safety and low toxic effect of YLSPS reported by a previous study [19].

The present study has revealed the anti-lung cancer mechanism of YLSPS, but TCM exerts its effect via multiple pathways and targets. There are some limitations since only the EMT process of lung cancer cells was investigated, and whether YLSPS has other regulatory effects

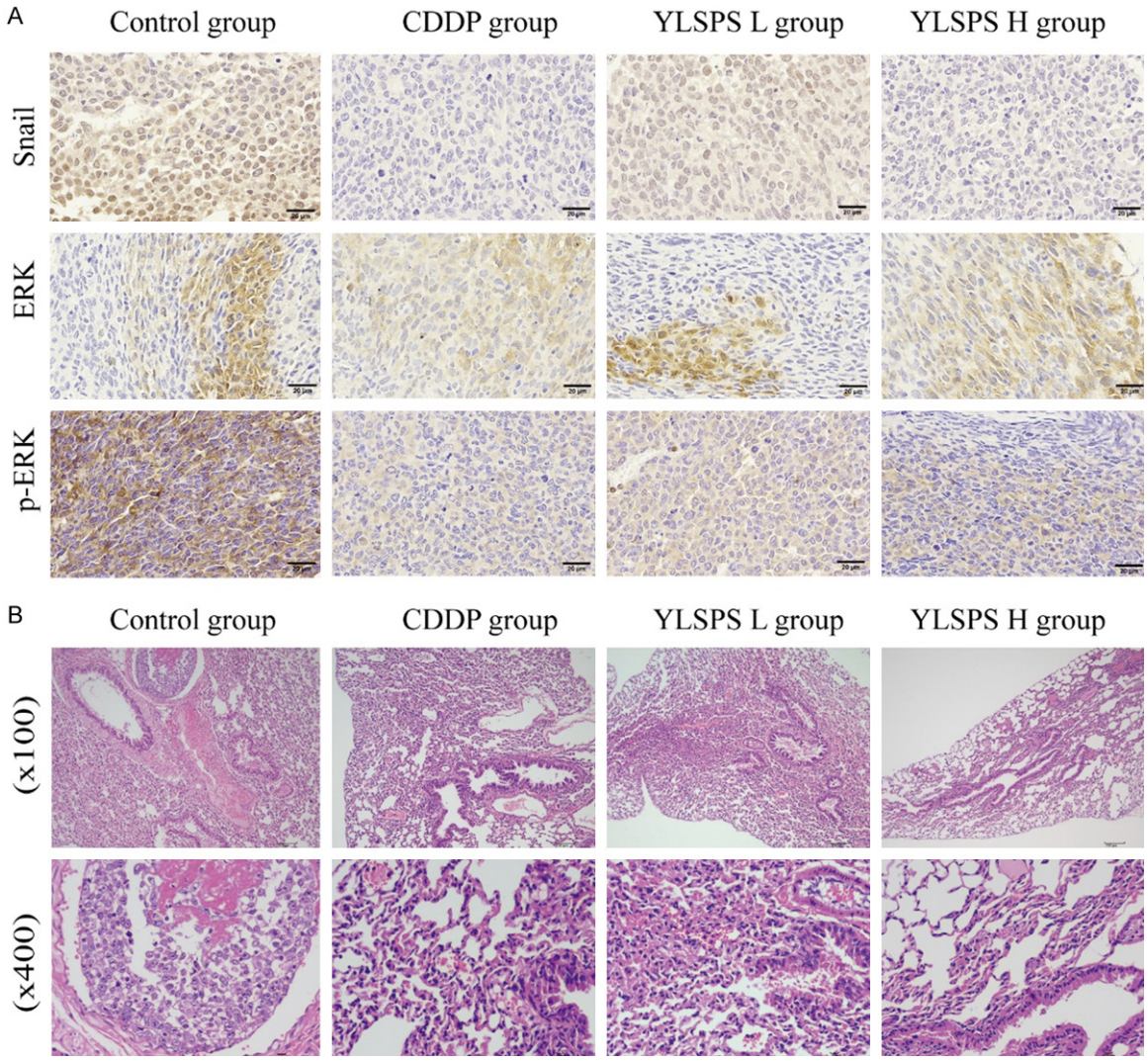

Figure 8. Expression of Snail, ERK and phosphorylated ERK by immunohistochemical staining (Scale bar =20 μm) (A). Histological observations of lung tissues by hematoxylin and eosin staining (magnification: ×100, ×400) (B).

on the tumor immune microenvironment needs to be further explored. Second, the current study only verified the effect of YLSPS on lung cancer migration and invasion and did not investigate the effect of YLSPS on TGF-β-mediated immunosuppression in depth. In addition, an animal model of spontaneous lung cancer metastasis needs to be established, and the mechanism by which YLSPS regulates the EMT process and tumor microenvironment of lung cancer *in vivo* needs to be further evaluated.

In summary, the results of the present study demonstrated for the first time that YLSPS could restrain EMT through the TGF-β1/ERK signaling pathway, inhibiting lung cancer cell migration and invasion. In addition, the mechanism by which YLSPS regulates the tumor microenvironment and exerts its antitumor effects in combination with other tumor treatment modalities, such as radiotherapy, chemotherapy, thermotherapy and immunotherapy, deserves further investigation.

Acknowledgements

The present study was supported by the Guangxi TCM Suitable Technology Development and Extension project (GZSY21-57) and the Scientific Research and Technology Development Program of Guangxi (NO. AB18221080).

Disclosure of conflict of interest

None.

Address correspondence to: Wenqi Liu, Department of Radiation Oncology, The Second Affiliated Hospital of Guangxi Medical University, Nanning 530007, Guangxi, China. Tel: +86-13517681161; E-mail: liuwenqigx@163.com; Renbin Huang, Pharmaceutical College, Guangxi Medical University, Nanning 530021, Guangxi, China. Tel: +86-0771-5358272; E-mail: huangrenbin518@163.com

References

[1] Siegel RL, Miller KD and Jemal A. Cancer statistics, 2020. CA Cancer J Clin 2020; 70: 7-30.
[2] Zhang XC, Wang J, Shao GG, Wang Q, Qu X, Wang B, Moy C, Fan Y, Albertyn Z, Huang X, Zhang J, Qiu Y, Platero S, Lorenzi MV, Zudaire E, Yang J, Cheng Y, Xu L and Wu YL. Comprehensive genomic and immunological characterization of Chinese non-small cell lung cancer patients. Nat Commun 2019; 10: 1772.
[3] Du L, Waqar SN and Morgensztern D. Multimodality therapy for NSCLC. Cancer Treat Res 2016; 170: 151-163.
[4] Tsai JH and Yang J. Epithelial-mesenchymal plasticity in carcinoma metastasis. Genes Dev 2013; 27: 2192-2206.
[5] Brabletz T. To differentiate or not--routes towards metastasis. Nat Rev Cancer 2012; 12: 425-436.
[6] Nieto MA, Huang RY, Jackson RA and Thiery JP. EMT: 2016. Cell 2016; 166: 21-45.
[7] Kraljevic Pavelic S, Sedic M, Bosnjak H, Spaventi S and Pavelic K. Metastasis: new perspectives on an old problem. Mol Cancer 2011; 10: 22.
[8] Massagué J. TGF-beta signal transduction. Annu Rev Biochem 1998; 67: 753-791.
[9] Fuxe J and Karlsson MC. TGF-β-induced epithelial-mesenchymal transition: a link between cancer and inflammation. Semin Cancer Biol 2012; 22: 455-461.
[10] Lin X, Jiang GN, Jiao Y, zhang J, Li J and Huang B. Chemical composition of Cliffbean polysaccharid. Chinese Traditional Patent Medicine 2009; 20: 901-902.
[11] Duan X, Jiao Y, Zhang S, Lu X and Huang R. Effects of Yulangsan polysaccharide on proliferation and collagen I production of hepatic stellate cells. China J Mod Med 2008; 4: 423-425.
[12] Huang J, Nguyen V, Tang X, Wei J, Lin X, Lai Z, Doan V, Xie Q and Huang R. Protection from diclofenac-induced liver injury by Yulangsan polysaccharide in a mouse model. J Ethnopharmacol 2016; 193: 207-213.
[13] Nguyen V, Huang J, Doan V, Lin X, Tang X, Huang Y, Tang A, Yang X and Huang R. Hepatoprotective effects of Yulangsan polysaccharide against nimesulide-induced liver injury in mice. J Ethnopharmacol 2015; 172: 273-280.
[14] Ruan W, Duan W, Liang X, Chen Z and Huang R. Protective effect of Yulangsan polysaccharide against hepatic injury in mice. Herald of Medicine 2015; 866-870.
[15] Cai W, Zhang X, Huang R and Wang N. Study on immunological effect of Yulangsan polysaccharides. Lishizhen Medicine and Materia Medica Research 2011; 22: 1681-1683.
[16] Zhen L, Teng L, Ren BH, Chun XC, Qing QC and Jin BW. Effect of Yulangsan polysaccharides on immune function of immunosuppressive mice induced by cyclophosphamide. Nat Prod Res Dev 2014; 26: 666.
[17] Liang S, Huang R, Lin X, Huang J, Huang Z and Liu H. Effects of Yulangsan polysaccharide on monoamine neurotransmitters, adenylate cyclase activity and brain-derived neurotrophic factor expression in a mouse model of depression induced by unpredictable chronic mild stress. Neural Regen Res 2012; 7: 191-196.
[18] Lin X, Huang Z, Chen X, Rong Y, Zhang S, Jiao Y, Huang Q and Huang R. Protective effect of Millettia pulchra polysaccharide on cognitive impairment induced by D-galactose in mice. Carbohydr Polym 2014; 101: 533-543.
[19] Chen C, Nong Z, Meng M, Wen Q, Lin X, Qin F, Huang J and Huang R. Toxicological evaluation of Yulangsan polysaccharide in Wistar rats: a 26-week oral gavage study. Environ Toxicol Pharmacol 2016; 41: 1-7.
[20] Cai W, Lin X, Zhang X, Zhang X, Wang N and Huang R. Influence of Yulangsan polysaccharide on apoptosis of human hepatoma cell line BEL7404. Chin J New Drugs Clin Rem 2008; 27: 332-335.
[21] Cai W, Chen X, Pan Q, Zhang S, Tan L, Sun X, Huang R and Xia A. Antitumor activity of Yulangsan polysacchrides in mice bearing S180 sarcoma tumors. Mol Clin Oncol 2017; 7: 716-720.
[22] Cai W, Zhang Z, Wang N, Zhang X and Huang R. Antitumor effect of Yulangsan polysaccharides in vivo. Chin J New Drugs Clin Rem 2010; 29: 119-122.
[23] Qin N, Lu S, Chen N, Chen C, Xie Q, Wei X, Ye F, He J, Li Y, Chen L, Jiang L, Lu X, Yuan Y, Li J, Jiao Y and Huang R. Yulangsan polysaccharide inhibits 4T1 breast cancer cell proliferation and induces apoptosis in vitro and in vivo. Int J Biol Macromol 2019; 121: 971-980.
[24] Li H, Su J, Jiang J, Li Y, Gan Z, Ding Y, Li Y, Liu J, Wang S and Ke Y. Characterization of polysaccharide from Scutellaria barbata and its antagonistic effect on the migration and invasion

of HT-29 colorectal cancer cells induced by TGF-β1. Int J Biol Macromol 2019; 131: 886-895.
[25] Shi S, Zhao J, Wang J, Mi D and Ma Z. HPIP silencing inhibits TGF-β1-induced EMT in lung cancer cells. Int J Mol Med 2017; 39: 479-483.
[26] Wu Y, Xu X, Ma L, Yi Q, Sun W and Tang L. Calreticulin regulates TGF-β1-induced epithelial mesenchymal transition through modulating Smad signaling and calcium signaling. Int J Biochem Cell Biol 2017; 90: 103-113.
[27] Shao N, Xiao Y, Zhang J, Zhu Y, Wang S and Bao S. Modified Sijunzi decoction inhibits epithelial-mesenchymal transition of non-small cell lung cancer by attenuating AKT/GSK3β pathway in vitro and in vivo. Front Pharmacol 2022; 12: 821567.
[28] Tang H, Huang W, Ma J and Liu L. SWOT analysis and revelation in traditional Chinese medicine internationalization. Chin Med 2018; 13: 5.
[29] Ling CQ, Yue XQ and Ling C. Three advantages of using traditional Chinese medicine to prevent and treat tumor. J Integr Med 2014; 12: 331-335.
[30] Yoder LH. Let's talk 'cancer prevention'. Medsurg Nurs 2005; 14: 195-198.
[31] Lamouille S, Xu J and Derynck R. Molecular mechanisms of epithelial-mesenchymal transition. Nat Rev Mol Cell Biol 2014; 15: 178-196.
[32] Marcucci F, Stassi G and De Maria R. Epithelial-mesenchymal transition: a new target in anticancer drug discovery. Nat Rev Drug Discov 2016; 15: 311-325.
[33] Gonzalez DM and Medici D. Signaling mechanisms of the epithelial-mesenchymal transition. Sci Signal 2014; 7: re8.
[34] Zhang J, Tian XJ and Xing J. Signal transduction pathways of EMT induced by TGF-β, SHH, and WNT and their crosstalks. J Clin Med 2016; 5: 41.
[35] Hua W, Ten Dijke P, Kostidis S, Giera M and Hornsveld M. TGFβ-induced metabolic reprogramming during epithelial-to-mesenchymal transition in cancer. Cell Mol Life Sci 2020; 77: 2103-2123.
[36] Wu Q, Li G, Wen C, Zeng T, Fan Y, Liu C, Fu GF, Xie C, Lin Q, Xie L, Huang L, Pu P, Ouyang Z, Chan HL, Zhao TJ, Chen XL, Fu G and Wang HR. Monoubiquitination of p120-catenin is essential for TGFβ-induced epithelial-mesenchymal transition and tumor metastasis. Sci Adv 2020; 6: eaay9819.
[37] Ramos C, Becerril C, Montaño M, García-De-Alba C, Ramírez R, Checa M, Pardo A and Selman M. FGF-1 reverts epithelial-mesenchymal transition induced by TGF-{beta}1 through MAPK/ERK kinase pathway. Am J Physiol Lung Cell Mol Physiol 2010; 299: L222-231.
[38] Jarrold J and Davies CC. PRMTs and arginine methylation: cancer's best-kept secret? Trends Mol Med 2019; 25: 993-1009.
[39] Batlle E and Massagué J. Transforming growth factor-β signaling in immunity and cancer. Immunity 2019; 50: 924-940.
[40] De Luca A, Maiello MR, D'Alessio A, Pergameno M and Normanno N. The RAS/RAF/MEK/ERK and the PI3K/AKT signalling pathways: role in cancer pathogenesis and implications for therapeutic approaches. Expert Opin Ther Targets 2012; 16 Suppl 2: S17-27.
[41] Yang SH, Sharrocks AD and Whitmarsh AJ. MAP kinase signalling cascades and transcriptional regulation. Gene 2013; 513: 1-13.
[42] Miao JX, Wang JY, Li HZ, Guo HR, Dunmall LSC, Zhang ZX, Cheng ZG, Gao DL, Dong JZ, Wang ZD and Wang YH. Promising xenograft animal model recapitulating the features of human pancreatic cancer. World J Gastroenterol 2020; 26: 4802-4816.
[43] Qin N, Chen N, He J, Huang R and Jiao Y. Acute toxicity of Yulangsan polysaccharides and its combination with cyclophosphamide in mice. The Chinese Journal of Clinical Pharmacology 2017; 33: 2287-2290.